Supporting Information

27-plex Tandem Mass Tag Mass Spectrometry for Profiling Brain Proteome in Alzheimer's Disease

Zhen Wang[1,5], Kaiwen Yu[1,5], Haiyan Tan[2,5], Zhiping Wu[1], Ji-Hoon Cho[2], Xian Han[1,3], Huan Sun[1],

Thomas G. Beach[4], Junmin Peng*[,1,2]

[1]Departments of Structural Biology and Developmental Neurobiology, St. Jude Children's Research Hospital, Memphis, TN 38105, USA

[2]Center for Proteomics and Metabolomics, St. Jude Children's Research Hospital, Memphis, TN 38105, USA

[3]University of Tennessee Health Science Center, Memphis, TN 38163, USA

[4]Banner Sun Health Research Institute, Sun City, AZ 85351, USA

[5]Contribute equally

*Correspondence: junmin.peng@stjude.org

Table of contents

Supporting results

Supporting methods

Table S1. Summary of human cases used in this study

Table S2. Differentially expressed (DE) proteins between normal and Alzheimer's disease (AD) postmortem brain samples

Figure S1. Evaluation of TMT27 performance in four different fraction conditions of basic pH LC

Figure S2. Quantification of mouse brain lysate

Figure S3. Comparison of the retention time of peptides labeled by TMT16 and TMT11

Figure S4. Optimization of normalized collision energy (NCE) for TMT16 and TMT11

Figure S5. Basic pH RPLC chromatograms of individual TMT11- and TMT16- labeled peptides from the similar set of protein samples

Figure S6. Peptides overlap comparison between individual TMT11/TMT16 and TMT27 or between TMT11 and TMT16 within TMT27.

Figure S7. Comparison of TMT27 with other hybrid high multiplexing methods.

Figure S8. Overview of the representative isobaric labeling reagents

Supporting references

Supporting results

Hydrophobicity and RPLC retention time analysis of TMT16 labeled peptides

As the TMT16 reagents have a longer hydrophobic linker than the TMT11 reagents, TMT16-labeled peptides are expected to be more hydrophobic than TMT11-labeled counterparts, resulting in different retention time (RT) in reverse-phase liquid chromatography (RPLC). To examine this point, we equally mixed TMT11- and TMT16-labeled peptides for a single LC-MS/MS run, and then analyzed the retention time shift (ΔRT) between TMT16- and TMT11-labeled peptides. For example, the extracted chromatograms of a representative peptide (GLSATVTGGQK with two TMT labeling sites, N-terminus and Lys) showed ΔRT of 7.5 min (**Fig. S3A**).

To investigate the ΔRT of all detected peptides, we focused on the peptides with two TMT labeling sites and plotted the ΔRT of each peptide along RT with the elution gradient of buffer B (**Fig. S3B**). Interestingly, we found that ΔRT showed a positive correlation with RT before about 30 min, but a negative correlation after 30 min (**Fig. S3B**). Since RT exhibited a good linear correlation with hydrophobicity (**Fig. S3C**), the relationship between ΔRT and RT can be explained by different effects of TMT16 tag on the hydrophobicity of various peptides. Namely, for the peptides of high hydrophobicity (eluted after 30 min), the higher hydrophobic they are, the less effect TMT16 tag has. On the other side, for these peptides of low hydrophobicity and high hydrophilicity (e.g., eluted before 30 min), the more hydrophilic they are, the less impact TMT16 tag has. In contrast, for these peptides eluted around 30 min, they are neither of high hydrophobicity nor of high hydrophilicity, the TMT16 tag displays the maximal influence on their RT. Consistent with this perspective, the ΔRT and peptide hydrophobicity index showed exactly the same relationship in the plotted curve (**Fig. S3D**). Similar results were obtained for the peptides with one TMT labeling site (i.e., Arg-ended tryptic peptides with only N-terminal amino group, **Fig. S3E-3F**). In total, 96% of TMT peptides have more than 0.5 min of ΔRT, which

indicates almost all the TMT16-labeled peptides can be well separated from TMT11-labeled peptides in acid pH RPLC.

In conclusion, TMT16 has a strong ΔRT effect on the peptides of intermediate hydrophobicity but shows a small ΔRT effect on the peptides with extremely high or low hydrophobicity. Thus, the starting and ending buffer B concentrations in the LC gradient are not significantly affected by the selection of different TMT labeling reagents, which is in contrast to our intuitive expectation that TMT16-labled peptides might require higher buffer B elution than TMT11-labeled peptides.

Supporting methods

Protein extraction, quantification and digestion

Human and mouse brain samples were lysed by vortexing in lysis buffer (50 mM HEPES, pH 8.5, fresh 8 M urea, and 0.5% sodium deoxycholate) with the addition of glass beads (100 μL lysis buffer and ~20 μL beads for 10 mg tissue)) as previously described[1]. The protein concentration was estimated by a Coomassie-stained short SDS gel with BSA as a standard[2]. The protein samples (~100 μg per sample) were digested with Lys-C (Wako, 1:100 w/w) at room temperature (RT) for 3 h, diluted with 50 mM HEPES (pH 8.5) to decrease urea to 2 M, and further digested by trypsin (Promega, 1:50 w/w) at RT overnight. The digested peptides were reduced by fresh dithiothreitol (DTT, 1 mM) for 2 h, alkylated by iodoacetamide (IAA, 10 mM) at dark for 30 min, and further quenched with DTT (30 mM) for 30 min. The peptides were acidified by adding trifluoroacetic acid (TFA) to 1% and centrifuged at 21,000 × g for 10 min to remove pellets. Each supernatant was desalted with a C18 Ultra-Micro SpinColumn (Harvard apparatus) using the standard protocol and peptide eluate was dried by speedvac. The

concentration of desalted peptides was further quantified by measuring the absorbance at 205 nm by the NanoDrop™ 2000c spectrophotometer (Thermo Fisher Scientific).

TMT labeling of the human brain samples

Human peptide samples were resuspended in 50 mM HEPES, pH 8.5 (~1 µg/µL), and divided into two aliquots. One aliquot was labeled with TMTpro reagents (termed TMT16) with TMT/protein ratio (w/w) of 1.5:1 for 30 min, including a collection of 16 samples (8 ADs, 7 controls, and 1 internal reference of a mixture of human brain samples). The other aliquot was labeled with TMT11 with TMT/protein ratio (w/w) of 1:1 for 30 min, including 11 samples (5 ADs, 5 controls, and 1 internal reference). The labeled samples were quenched with 0.5% hydroxylamine for 15 min.

Pooling of 11-plex, 16-plex and 27-plex samples

To obtain equal pooling of TMT11 samples, we performed the experiment in the following steps. First, half of each TMT11 sample was pre-mixed, and a small aliquot (~1 µg) was desalted and quantified by LC-MS/MS. Then we adjusted the amount of the pre-mixed sample by adding the individual remaining samples to reach the equal TMT11 pool. The TMT16 pool was made by the same procedure. The TMT11 pool and the TMT16 pool were divided into a total of four aliquots (two for each pool), in which two aliquots were used for individual 11-plex and 16-plex analyses, while the other two aliquots were mixed for the 27-plex analysis.

Optimization of desalting conditions for the TMT16 peptides

The mouse brain peptide sample (600 µg) was labeled with TMT16zero and acidified by adding TFA to 1% after quenching, followed by centrifugation at 21,000 × g for 10 min. The supernatant was equally divided and loaded on six pre-equilibrated C18 Ultra-Micro SpinColumn Ultra-C18 Micro spin columns. The columns were spun at 100 × g for 3 min to collect flow-through, and then washed three times under six different conditions (5 or 10 bed volumes of 0.1% TFA plus

0%, 2.5%, or 5.0% AcN). The peptides were eluted with 5 bed volumes of elution buffer (60% AcN and 0.1% TFA) and dried by speedvac for further LC-MS/MS analysis. Based on the MS results, the condition of 10 bed volumes of 0.1% TFA plus 5% AcN was selected for desalting of TMT samples.

Basic pH LC fractionation

The pooled peptide samples of 11-plex, 16-plex and 27-plex were fractionated by an offline basic pH RPLC with XBridge C18 column (3.5 μm particle size, 2.1 mm × 15 cm, Waters; buffer A: 10 mM ammonium formate, pH 8.0; buffer B: 90% AcN, 10 mM ammonium formate, pH 8.0). The peptides were eluted in a 160 min gradient of 15-42% buffer B, and 160 fractions were collected every min and concatenated to 40 fractions.

Cell type correction

Protein changes may be caused by the change of different populations of cell types in heterogeneous brain samples. We then performed cell type correction to normalize this confounding factor as previously described[3]. Briefly, we corrected protein abundance by the cell type composition, including four cell types (neurons, astrocytes, microglia, and oligodendrocytes). Cell type protein markers were identified based on the published cell-type-specific proteome[4]. The change of each cell type was evaluated as the median of protein abundance of all identified cell type markers. The corrected proteomic dataset was used for downstream differential expression (DE) and pathway analyses.

Protein identification and quantification by JUMP software

Protein identification was performed by JUMP search engine[5]. The protein database was generated by combining downloaded Swiss-Prot, TrEMBL, and UCSC databases and removing redundancy (human: 83,955 entries; mouse: 59,423 entries). The target protein sequences were reversed to generate a decoy database to evaluate the false discovery rate (FDR)[6]. Major

parameters included 6 ppm mass tolerance for precursor and 15 ppm for product ions, full trypticity, and two maximal missed cleavages. Cys carbamidomethylation (+57.02146) and TMT modification of Lys and N-termini (+229.16293 for TMT11 or +304.20715 for TMT16) were set as static modifications. Oxidation of Met (+15.99491) was set as a dynamic modification. The resulting PSMs were filtered by mass accuracy and then grouped by precursor ion charge state followed by the cutoffs of JUMP-based matching scores (Jscore and ΔJn) to reduce FDR below 1% for proteins. When the same peptide was derived from numerous homologous proteins, the peptide was matched to the protein with the top PSM number, according to the rule of parsimony. In TMT27 datasets, the same PSMs which matched to both TMT11- and TMT16-labeled peptides suggested a mixed spectra and were removed. The protein quantification was performed using the TMT reporter ion intensities with the reported method with y1-ion based correction of TMT data[7]. The raw data of 27-plex were processed to obtain TMT11 and TMT16 datasets separately.

Calculation of peptide hydrophobicity index

The TMT11-labeled peptide hydrophobicity index was predicted using the Sequence Specific Retention Calculator (Version Q) based on the reported algorithm[8].

Differential expression and pathway enrichment analyses

The analysis was performed following the previously reported protocol[3]. Briefly, individual protein intensities in each dataset were normalized using the internal reference and the redundancy was removed. The protein intensities of the same sample quantified in 11-plex, 16-plex and 27-plex datasets were averaged. Then the measurement variation was analyzed according to the replicated measurements. The ratios of all proteins between the replicates were modeled with a Gaussian distribution to evaluate standard deviation (SD) for z value analysis. The protein p values were obtained by using the moderated t-test[9] and were further

corrected by Benjamini-Hochberg correction for multiple testing. The proteins with adjusted *p*-value (FDR) < 0.1 and at least 2-fold of the standard deviation (z > 2) were considered as DE proteins. Pathway enrichment analysis based on the functional annotation of the DE proteins was performed using the online Database for Annotation, Visualization and Integrated Discovery (DAVID 6.8, https://david.ncifcrf.gov/).
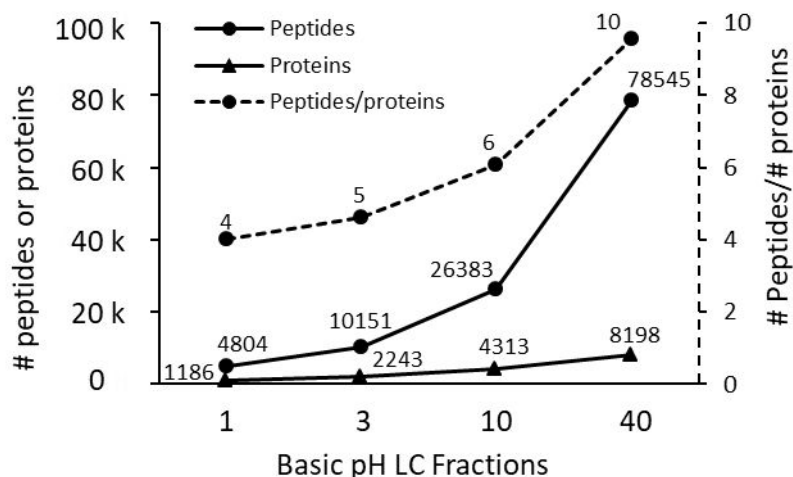
Figure S1. Evaluation of TMT27 performance in four different fraction conditions of basic pH LC. 1, 3, 10 or 40 fractions were selected. The average numbers of peptides and proteins identified in internal TMT11- and TMT16-labeled datasets are shown. The dashed curve plots the ratio between peptides and proteins under each condition.
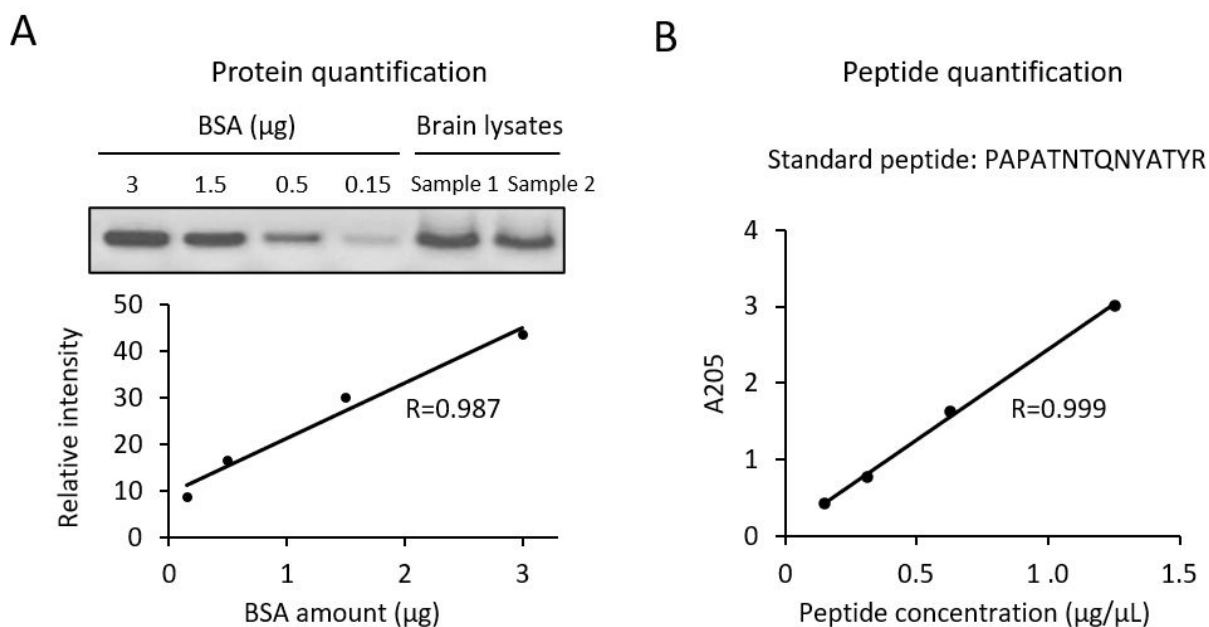

Figure S2. Quantification of mouse brain lysate. (A) Quantification of mouse brain lysate on a short SDS gel with BSA as standard. The standard curve graphs the BSA concentration and Coomassie-stained protein band intensity used for quantification. (B) Peptide quantification by NanoDrop UV-Vis spectrophotometers using the absorbance at 205 nm. The synthetic peptide PAPATNTQNYATYR was used to make the standard curve for peptide quantification.
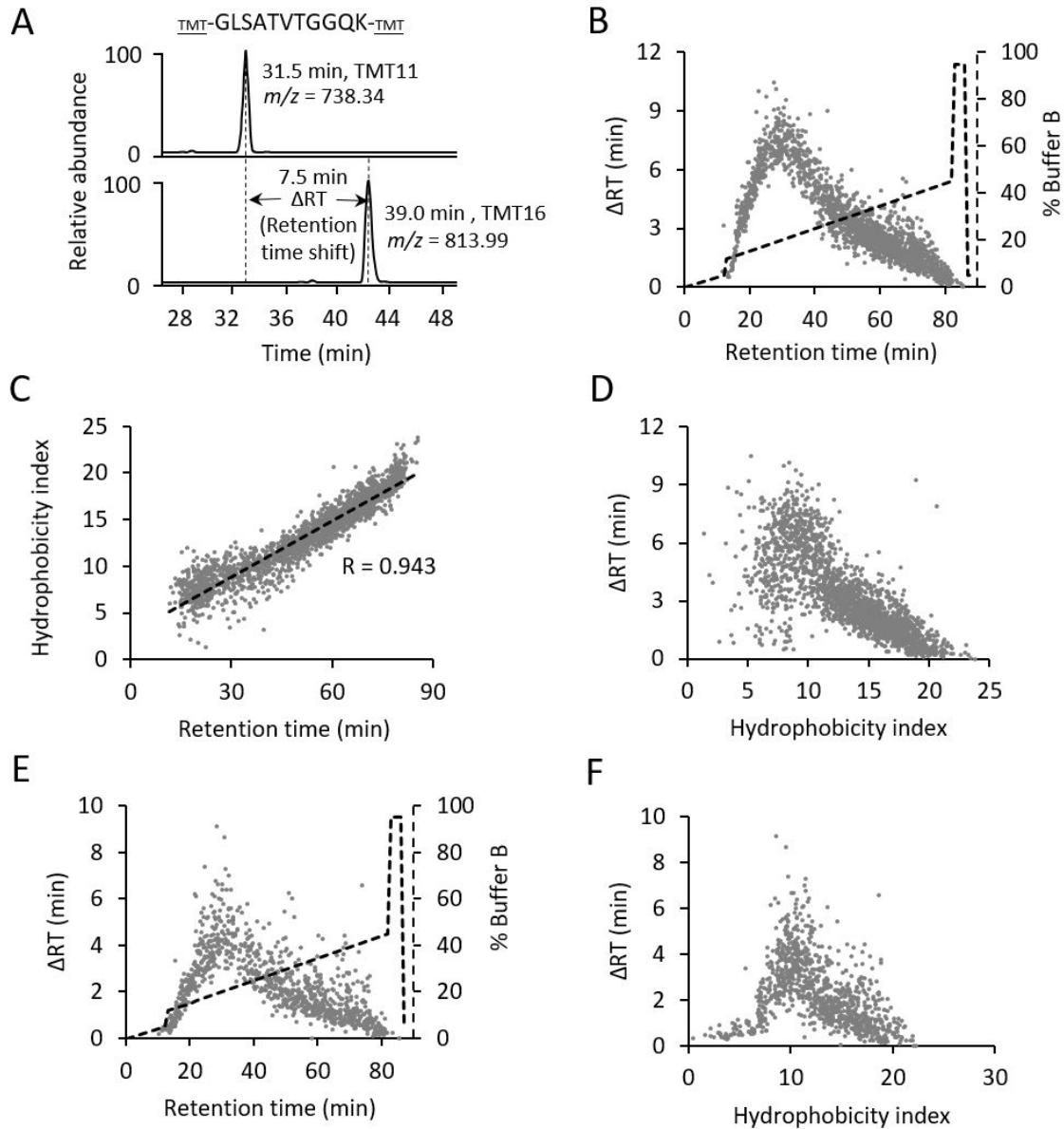
Figure S3. Comparison of the retention time of peptides labeled by TMT16 and TMT11. TMT11- and TMT16-labeled peptides were mixed equally, the mixture was analyzed by LC-MS/MS. The overlapped peptides with two TMT labeling sites were used for further analyses in (A-D) and the overlapped peptides with one labeling site were analyzed in (E-F). (A) Extracted ion chromatograms of the peptide GLSATVTGGQK labeled by TMT11 and TMT16 with retention time shift (ΔRT) are shown. (B) The relationship between two TMT-labeled peptide retention time and ΔRT. The gradient of buffer B after correction of dead volume is aligned in the same plot. (C) Correlation analysis between two TMT11-labeled peptide retention time and hydrophobicity index. (D) The relationship between two TMT-labeled peptide hydrophobicity index and ΔRT. (E) The relationship between one TMT-labeled peptide retention time and ΔRT. The gradient of buffer B after correction of dead volume is aligned in the same plot. (F) The relationship between one TMT-labeled peptide hydrophobicity index and ΔRT.
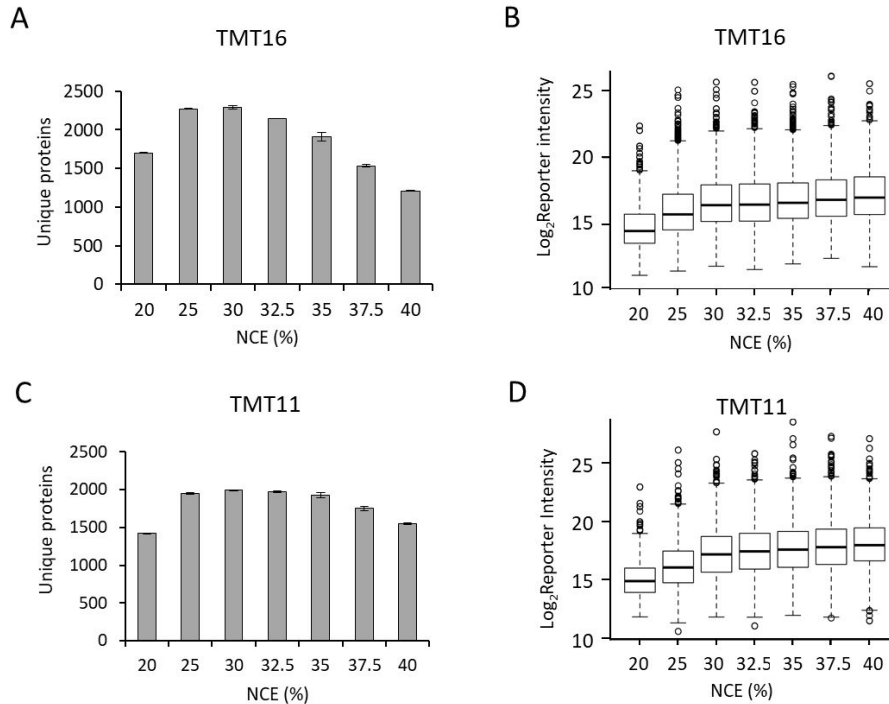
Figure S4. Optimization of normalized collision energy (NCE) for TMT16- and TMT11-labeled peptides. (A) and (C) Identified unique protein numbers in individual TMT16- or TMT11-labeled samples under various NCE conditions. (B) and (D) Box plots showing the distributions of the reporter ion intensities (internal reference channel) in the TMT16- or TMT11-labeled samples under distinct NCE conditions.
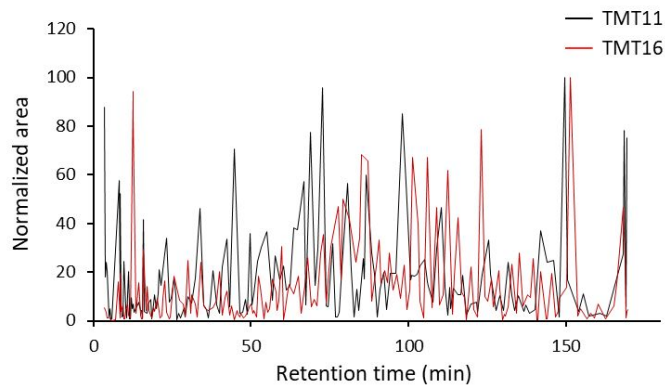

Figure S5. Basic pH RPLC chromatograms of individual TMT11- and TMT16-labeled peptides from the similar set of protein samples.

A Unique peptides
TMT11 TMT11 in TMT27
70,045 — 71,123 — 8,909

B Unique peptides
TMT16 TMT16 in TMT27
52,923 — 69,960 — 10,100

C Unique peptides
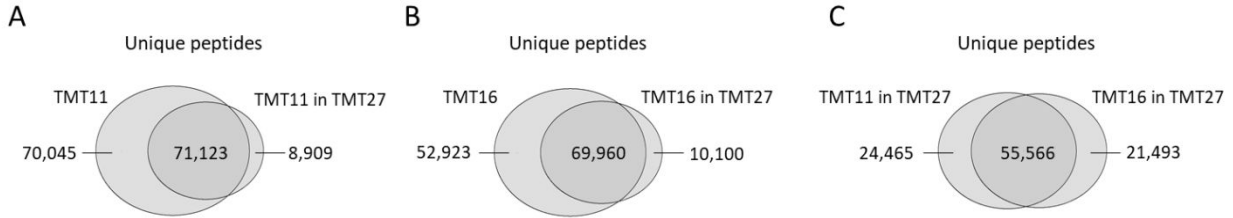TMT11 in TMT27 TMT16 in TMT27
24,465 — 55,566 — 21,493

Figure S6. Peptide comparison among individual TMT11 and TMT16 datasets and internal TMT11 and TMT16 datasets within TMT27. (A) The Venn diagram indicates the overlapped TMT11-labeled peptides identified in the TMT11 and TMT27 methods. (B) The Venn diagram shows the overlapped TMT16-labeled peptides identified in the TMT16 and TMT27 methods. (C) The Venn diagram presents the overlapped internal TMT11- and TMT16-labeled peptides in the TMT27 experiment.

Method	Pros	Con
TMT27	• Use similar chemical labeling tags making the experiment easy to process. • Only need one-step labeling. • Can be applied to any biological samples.	• Increase the complexity of reporter ions, which may lead to ratio compression if peptide fractionation is limited.
SILAC + TMT/iTRAQ	• Combine with SILAC allow accurate quantitation. • May use a multiplexed SILAC method.	• Restrict by the metabolic labeling in the SILAC method (e.g. difficult to apply to clinical samples) • Need two-step labeling.
cPILOT (dimethyl + isobaric)	• Lower costs as the dimethylation reagents are inexpensive compared to other isobaric reagents. • Can be applied to any biological samples.	• Need two-step labeling. • Require stringent conditions to firstly label N-termini by the dimethyl group, and then label Lys by isobaric tags. • Quantify only Lys-containing peptides.

Figure S7. Comparison of TMT27 with other hybrid high multiplexing methods (SILAC combing with TMT/iTRAQ, and cPILOT).
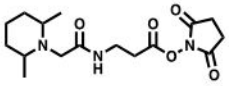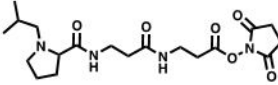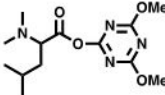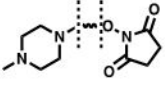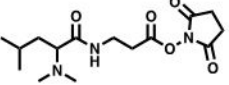
Isobaric tag structure	Added mass	Reporter ion mass	
TMT 11-plex	229.16293	126.12773 127.12476 127.13108 128.12812 128.13444 129.13147	129.13779 130.13483 130.14115 131.13818 131.14450
TMT 16-plex	304.20715	126.12773 127.12476 127.13108 128.12812 128.13444 129.13147 129.13779 130.13483	130.14115 131.13818 131.14450 132.14154 132.14786 133.14489 133.15121 134.14825
DiLeu 12-plex	145.12000 145.12632 145.13216 145.12831 145.13463 145.14047	115.12476 115.13108 116.12812 116.13444 116.14028 117.13147	117.13731 117.14363 118.13483 118.14067 118.14699 118.15283
iTRAQ 8-plex	304.20536 304.19904	113.10733 114.11068 115.10772 116.11107	117.11442 118.11146 119.11481 121.12152
DiART 6-plex	216.15511 216.14879 216.16095 216.15463 216.17312 216.16680	114.12773 115.12476 116.14028 117.13731 118.15283 119.14987	

Figure S8. Overview of the representative isobaric labeling reagents.

Supporting references

1.   Bai, B.; Tan, H.; Pagala, V. R.; High, A. A.; Ichhaporis, V. P.; Hendershot, L.; Peng, J., Deep profiling of proteome and phosphoproteome by isobaric labeling, extensive liquid chromatography, and mass spectrometry. *Methods Enzymol.* **2017,** *585*, 377-395.

2.   Xu, P.; Duong, D. M.; Peng, J. M., Systematical Optimization of Reverse-Phase Chromatography for Shotgun Proteomics. *J. Proteome Res.* **2009,** *8* (8), 3944-3950.

3.   Bai, B.; Wang, X.; Li, Y.; Chen, P.-C.; Yu, K.; Dey, K. K.; Yarbro, J. M.; Han, X.; Lutz, B. M.; Rao, S.; Jiao, Y.; Sifford, J. M.; Han, J.; Wang, M.; Tan, H.; Shaw, T. I.; Cho, J.-H.; Zhou, S.; Wang, H.; Niu, M.; Mancieri, A.; Messler, K. A.; Sun, X.; Wu, Z.; Pagala, V.; High, A. A.; Bi, W.; Zhang, H.; Chi, H.; Haroutunian, V.; Zhang, B.; Beach, T. G.; Yu, G.; Peng, J., Deep multilayer brain proteomics identifies molecular networks in Alzheimer's disease progression. *Neuron* **2020**.

4.   Sharma, K.; Schmitt, S.; Bergner, C. G.; Tyanova, S.; Kannaiyan, N.; Manrique-Hoyos, N.; Kongi, K.; Cantuti, L.; Hanisch, U.-K.; Philips, M.-A.; Rossner, M. J.; Mann, M.; Simons, M., Cell type– and brain region–resolved mouse brain proteome. *Nat. Neurosci.* **2015,** *18* (12), 1819-1831.

5.   Wang, X.; Li, Y.; Wu, Z.; Wang, H.; Tan, H.; Peng, J., JUMP: a tag-based database search tool for peptide identification with high sensitivity and accuracy. *Mol. Cell. Proteomics* **2014,** *13* (12), 3663-73.

6.   Peng, J.; Elias, J. E.; Thoreen, C. C.; Licklider, L. J.; Gygi, S. P., Evaluation of multidimensional chromatography coupled with tandem mass spectrometry (LC/LC-MS/MS) for large-scale protein analysis: the yeast proteome. *J. Proteome Res.* **2003,** *2* (1), 43-50.

7.   Niu, M.; Cho, J. H.; Kodali, K.; Pagala, V.; High, A. A.; Wang, H.; Wu, Z.; Li, Y.; Bi, W.; Zhang, H.; Wang, X.; Zou, W.; Peng, J., Extensive Peptide Fractionation and y1 Ion-Based Interference Detection Method for Enabling Accurate Quantification by Isobaric Labeling and Mass Spectrometry. *Anal. Chem.* **2017,** *89* (5), 2956-2963.

8.   Krokhin, O. V.; Craig, R.; Spicer, V.; Ens, W.; Standing, K. G.; Beavis, R. C.; Wilkins, J. A., An improved model for prediction of retention times of tryptic peptides in ion pair reversed-phase HPLC. *Mol. Cell. Proteomics* **2004,** *3* (9), 908.

9.   Phipson, B.; Lee, S.; Majewski, I. J.; Alexander, W. S.; Smyth, G. K., Robust hyperparameter estimation protects against hypervariable genes and improves power to detect differential expression. *Ann. Appl. Stat.* **2016,** *10* (2), 946-963.